The effect of bathymetric filtering on nearshore process model results

Nathaniel G. Plant [a,*], Kacey L. Edwards [b], James M. Kaihatu [c], Jayaram Veeramony [b], Larry Hsu [b], K. Todd Holland [b]

[a] U.S. Geological Survey, St. Petersburg FL 33701, United States
[b] Naval Research Laboratory, Stennis Space Center, MS 39529, United States
[c] Zachary Department of Civil Engineering, Texas A&M University, College Station, TX 77843, United States

ARTICLE INFO

ABSTRACT

Nearshore wave and flow model results are shown to exhibit a strong sensitivity to the resolution of the input bathymetry. In this analysis, bathymetric resolution was varied by applying smoothing filters to high-resolution survey data to produce a number of bathymetric grid surfaces. We demonstrate that the sensitivity of model-predicted wave height and flow to variations in bathymetric resolution had different characteristics. Wave height predictions were most sensitive to resolution of cross-shore variability associated with the structure of nearshore sandbars. Flow predictions were most sensitive to the resolution of intermediate scale alongshore variability associated with the prominent sandbar rhythmicity. Flow sensitivity increased in cases where a sandbar was closer to shore and shallower. Perhaps the most surprising implication of these results is that the interpolation and smoothing of bathymetric data could be optimized differently for the wave and flow models. We show that errors between observed and modeled flow and wave heights are well predicted by comparing model simulation results using progressively filtered bathymetry to results from the highest resolution simulation. The damage done by over smoothing or inadequate sampling can therefore be estimated using model simulations. We conclude that the ability to quantify prediction errors will be useful for supporting future data assimilation efforts that require this information.

Published by Elsevier B.V.

1. Introduction

Nearshore process models are capable of predicting both wave evolution across the nearshore region as well as the associated wave and wind driven nearshore currents (Booij et al., 1999; Reniers et al., 2007). Required input to this modeling approach includes estimates of water levels, wind, and a spectral description of the waves on the open boundaries as well as the bathymetry at all modeled locations. Our ability to describe these inputs is only as good as the technology used to measure and interpret them. For example, bathymetry is typically surveyed at discrete spatial locations and times as the data density is limited by the amount of time required to conduct the survey or to time periods where marine weather conditions permit survey operations. Bathymetric data will tend to be sparsely sampled in either space or time, and, therefore, it must be interpolated in order to fully populate model domains.

Furthermore, there is a potential (if not certain) mismatch between the scales that we wish to resolve with the nearshore process model (e.g., beach cusps, crescentic bars, and rip channels) and the scales that are resolved by the survey data (which may be higher or lower resolution than required, Plant et al., 2002). This mismatch is usually addressed through numerical treatment of the data (interpolation) or

the model (adjust grid resolution) or both. It is not clear which method or combination of methods yields the best model predictions. And, it is not clear that the optimal bathymetry for a particular wave model is also the optimal bathymetry for a corresponding flow model.

If we focus on the problem of providing bathymetry to a nearshore process model, then we would like to be able to objectively specify an optimal survey design to appropriately support a specific model resolution. This assumes that the important scales of variability have been selected by the modeler or model forecast user. Different users would likely have different requirements concerning the resolved scales in the model predictions. For instance, for public safety it might be important to resolve rip currents at hourly intervals with spacing of tens to hundreds of meters while for land-use management it might be important to resolve shoreline variations over years and decades spanning distances of tens to hundreds of kilometers. Using the model design as a constraint, the question becomes "what are the smallest spatial scales that a bathymetric survey needs to resolve in order to support an accurate model prediction?"

The answer to this question depends on properties of the environment as well as the model. For instance, if the spatial resolution of a particular model implementation is 10 m-by-10 m (cross-shore and alongshore dimensions), then the model will not resolve features with length scales shorter than 20 m-by-20 m (the Nyquist wave length). If such short scales exist in the real environment, they are assumed to be unimportant and they might need to be filtered out of the bathymetry

* Corresponding author. Tel.: +1 727 803 8747x3072; fax: +1 727 803 2032.
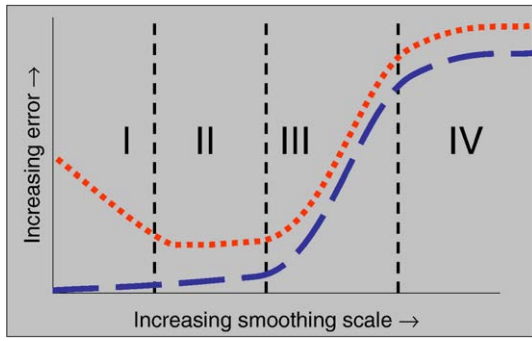E-mail address: nplant@usgs.gov (N.G. Plant).

Fig. 1. Idealized model error response to bathymetric smoothing. The dashed curve describes errors due to comparing a model with high-resolution bathymetry to a model with filtered bathymetry. The dotted line describes error between observations and a model with filtered bathymetry. The error regimes I–IV are described in the text.

that is used by the model to prevent aliasing that could lead to model errors. For instance, aliasing can cause short-scale beach cusps to masquerade as larger-scale rhythmic features (Plant et al., 2002). Even if the observations are sufficiently dense to resolve short scale features, there may be model errors if the processes associated with the short features are not accurately parameterized. As an example, the swash flow (and many other details) associated with short-scale beach cusps is not resolved by typical wave-averaged model schemes. Therefore, the beach cusps might need to be filtered out of the bathymetry unless processes associated with unresolved features are added to the model in the form of new parameterizations.

Our present hypothesis is that model errors can be minimized through some amount of bathymetric filtering and that the optimal amount of filtering should depend on the range of spatial scales that are accurately parameterized. Fig. 1 provides a qualitative picture of the effect that short scale variations and smoothing might have on model error. The modeled quantity of interest could be either wave height or flow velocity sampled at one or more locations. Consider a model-data comparison for the situation where the model grid resolution is held constant. Imagine that we have collected bathymetric data that are at much higher resolution than the model grid such that we could directly use surveyed depths at all locations within the model domain, if so desired. Assuming that short scale (compared to the model grid resolution) variations exist in the bathymetric data, we should more appropriately apply some sort of filtering to remove potential aliasing. We can apply a linear filter that takes the form

$$Z_{filt}(x_i, y_i, t_i) = \sum_j a_{ij} Z_{obs}(x_j, y_j, t_j), \tag{1}$$

where Z_{obs} is the observed bathymetry at discrete locations x_j, y_j, t_j, and Z_{filt} is the filtered bathymetry evaluated on the model domain (x_i, y_i, t_i). The filter weights take the functional form:

$$a_{ij} = \text{funct.}\left(\left|\frac{x_j - x_i}{L_x}\right| + \left|\frac{y_j - y_i}{L_y}\right| + \left|\frac{y_j - t_i}{L_t}\right|\right), \tag{2}$$

with smoothing scale parameters L_x, L_y, and L_t, where the subscripts x, y, and t correspond to cross-shore, alongshore, and time coordinates, respectively. The larger the smoothing scale, the more the output is filtered.

If the filter scale is much smaller than the distance between survey observations, then only one observation will contribute to the summation in Eq. (1). If the filter scale is also much smaller than the model grid spacing, then the model's bathymetry will include aliasing errors. We label model errors due to aliasing as type-I errors, which result if not enough filtering has been applied to the data. Type-I errors may also result if there is no aliasing, but, instead, the input bathymetry resolves short-scale features and associated processes that are not treated by the model (e.g., swash over beach cusps is not

treated by wave-averaged models). As the filter scale is increased, type-I errors are removed and we expect that the overall model performance will be improved. At this point, we achieve the smallest model errors (type-II errors) because the bathymetry is well matched to the scales that are resolved by the model. In this case, type-II errors reflect intrinsic model deficiencies that are not related to the bathymetry errors. If further smoothing does not affect model errors, then (1) there may be no significant bathymetric variations at these scales or (2) the model is intrinsically insensitive to these variations. At some point, the smoothing begins to remove the features that are important to the model prediction (type-III errors). For instance, sandbars or rip channels might be removed with large cross-shore or alongshore filter scales. Finally, all interesting features are removed at very large filter scales; the bathymetry is replaced by a planar or even horizontal surface, and additional filtering does not inflict much additional damage (type-IV errors).

An understanding of the sensitivity of model prediction errors can be used to identify optimal sampling strategies. Survey data that yield only type-II errors are desired. If the upper limit of the smoothing scale for this error type is known, then survey data need to be sampled to support this amount of filtering. This requires samples spaced about one-half the optimal smoothing scale (Plant et al., 2002).

It is not always possible to design an optimal survey. Then, the relevant question becomes "what damage does a particular survey resolution do to the model predictions?" Again, we have the option to filter the short scale bathymetric features in order to reduce model prediction errors, but important features may not be resolved. Without additional information, the best we can do is to estimate the errors that have crept into the problem. We would like to know what type of errors (types I–IV) will be encountered, and we would like to be able to quantify the error magnitudes. This knowledge can be used, for instance, in a data assimilation strategy. A typical application would be to find an optimal combination of model predictions and sparse in situ observations. For example, if both modeled and observed nearshore currents are available, the observations can be used to update the model prediction via a Kalman filter (Kalman, 1960). Consider assimilation of modeled and observed velocities (U_{model} and $U_{observed}$):

$$U_{update} = U_{model} + K(U_{observed} - U_{model})$$
$$K = \frac{\sigma_{model}^2}{\sigma_{observed}^2 + \sigma_{model}^2}. \tag{3}$$

Here σ describes model and observation errors. If the model error is relatively large, then K is large, and the updated velocity, U_{update}, is dominated by the observations. The important point is that both model and observation errors are required known in this type of optimal assimilation.

The objective of this paper is to estimate the sensitivity of nearshore hydrodynamic model errors to progressive filtering of the input bathymetry. We are treating the smoothness of the bathymetry as a control variable, much like other studies investigate the sensitivity of model results to the choice of parameterization or parameter value. We estimate errors in prediction of both wave height and mean current vectors and will show observed response to bathymetric smoothing that is consistent with Fig. 1. In Section 2 (Approach) we describe Duck94 (Birkemeier and Thornton, 1994) data collection, data processing, and Delft3D (Lesser et al., 2004) model implementation. In Section 3 (Results) we describe the model data error comparisons evaluated at a number of smoothing scales for several representative cases. We find that the flow and wave height errors have different sensitivity to smoothing and that these errors are predictable. Finally, in section 4 (Discussion and Conclusions) we comment on the implications that the results have on modeling, surveying, and assimilation. The conclusion is that the analysis approach presented here can be used to implement optimal survey

and model designs as well as facilitate optimal combination of model predictions and observations.

2. Approach

In order to evaluate the sensitivity of the nearshore wave height and flow velocity prediction errors to variations in the filtering scale applied to the input bathymetry, we need to find observations having relatively high resolution bathymetry, and we need corresponding observations of the wave height and flow velocities. The Duck94 field experiment included all of these measurements over several months. During this period, there was significant variation in the incident wave conditions and bathymetry. For our evaluation, we chose to analyze conditions on the 19th of October (1994) when moderate wave conditions resulted in strong gradients in the wave height (due to breaking over an offshore sandbar) and substantial nearshore flow velocities. In addition to a sandbar, the bathymetry included strong alongshore variability that also controlled the nearshore flow. Under these conditions, the flow could not be predicted well using a 1-dimensional profile modeling approach that requires alongshore uniform bathymetry (Ruessink et al., 2001). Thus, the problem must be studied with a 2-dimensional area model. The conditions that we chose to analyze contain sufficient hydrodynamic and bathymetric variability and, therefore, guarantee a strong model response to the application of progressive bathymetric filtering. This is an excellent test case for our analysis.

2.1. Bathymetry

The bathymetry data was surveyed from several vehicles, including the Coastal Research Amphibious Buggy (CRAB, Birkemeier and Mason, 1984) and a variety of hand-pushed or motorized vehicles used to survey the intertidal bathymetry with a differential global positioning system (Plant and Holman, 1997). Coastal process models require (a) spatially extensive bathymetry that (b) represents the true bathymetry at the simulation time and (c) satisfies model boundary condition requirements. (For example, a typical boundary condition requires alongshore gradients to vanish at the lateral boundaries.)
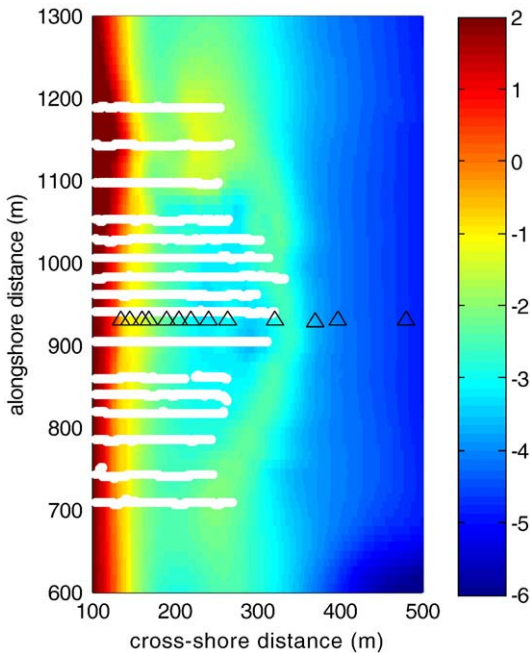

Fig. 2. Bathymetric surface estimated using data from 19 October 1994. White dots indicate survey sample locations and black triangles indicate wave and flow observation locations.
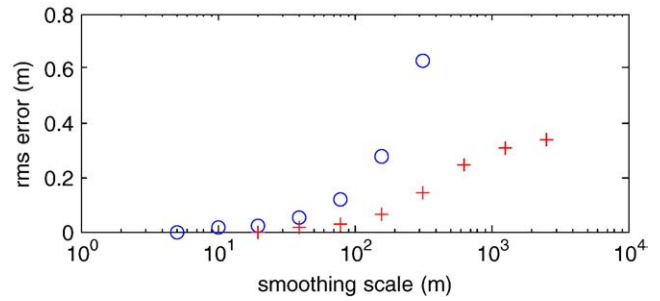

Fig. 3. Bathymetry errors as a function of cross-shore (o) and alongshore (+) smoothing scale. Variations in cross-shore filtering scale are shown with the alongshore filtering scale held at its smallest value (and vice-versa).

Since these conditions were not satisfied on the day selected for analysis (Fig. 2), we chose to solve this problem by constructing a composite bathymetry.

$$Z_3(x_i, y_i, t_i) = Z_1(x_i, y_i) + K_b(x_i, y_i, t_i)\{Z_2(x_i, y_i, t_i) - Z_1(x_i, y_i)\}, \quad (4)$$

where Z_1 is a spatially extensive but temporally invariant background bathymetry that satisfies boundary condition constraints and Z_2 the background bathymetry in the region that was surveyed on 19 October and also satisfies boundary conditions. Our approach is to first estimate Z_1 on a somewhat coarse grid, and then subtract this bathymetry from the data before estimating the perturbations, Z_2. The weights, K_b, are computed from known interpolation errors (Plant et al., 2002) as in Eq. (3) (replacing U_{model} with Z_1, $U_{observed}$ with Z_2, σ_{model} and $\sigma_{observed}$ with the corresponding interpolation errors).

The background bathymetry was interpolated using Eqs. (1)–(2) from 49 surveys with a total of 252,839 observations. The filter weights a_{ij} were evaluated using a Hanning filter (Press et al., 1992), and the smoothing scales were set to $L_x = 40$ m, $L_y = 100$ m, $L_t = 90$ days (Plant et al., 2002). To satisfy model boundary constraints, the bathymetry was forced to an alongshore-uniform surface within 200 m of the alongshore boundaries of the model domain using cubic B-splines (Ooyama, 1987). This background bathymetric surface (Z_1) was stored at a spatial resolution of $\Delta x = 10$ m and $\Delta y = 25$ m spanning a domain that was 1000 m wide in the cross-shore (x) direction and 1700 m wide in the alongshore (y) direction, centered on the so-called "mini-grid" region that was surveyed daily by the CRAB (Fig. 2).

Next, the perturbation bathymetry (Z_2) was interpolated at higher resolution with $L_x = 10$ m, $L_y = 40$ m, and $L_t = 2$ days in a domain that was 1000 m wide in the cross-shore, but only 700 m wide alongshore. This region corresponded to the location of the daily CRAB surveys, which provide data appropriate to the analysis date (19 October). Using B-splines, the boundaries were forced to the Z_1 bathymetry within 100 m of the edges of this domain. The perturbation bathymetry was saved at higher resolution than the background: $\Delta x = 2.5$ m, $\Delta y = 10$ m.

Our approach was to apply a range of filter scales to the Z_3 bathymetry, producing a series of Z_{filt} estimates, each corresponding to a different set of filter scales. Assuming that the original Z_3 bathymetry constructed as described above is the "true" bathymetry, we can construct an error plot that compares the unfiltered Z_3 to the filtered output (Fig. 3). The error in this case indicates the increasing damage that the filter operation inflicts on the bathymetry as the filter scales increase. Regions with rapid increase in error (e.g., 50 m < L_x < 500 m and 100 m < L_y < 1000 m) indicate regions where significant bathymetric variations (cross-shore and alongshore sandbar features) are removed. Our analyses included filtering scales of $L_x = 5, 10, 20, 40, 80, 160, 320$ m
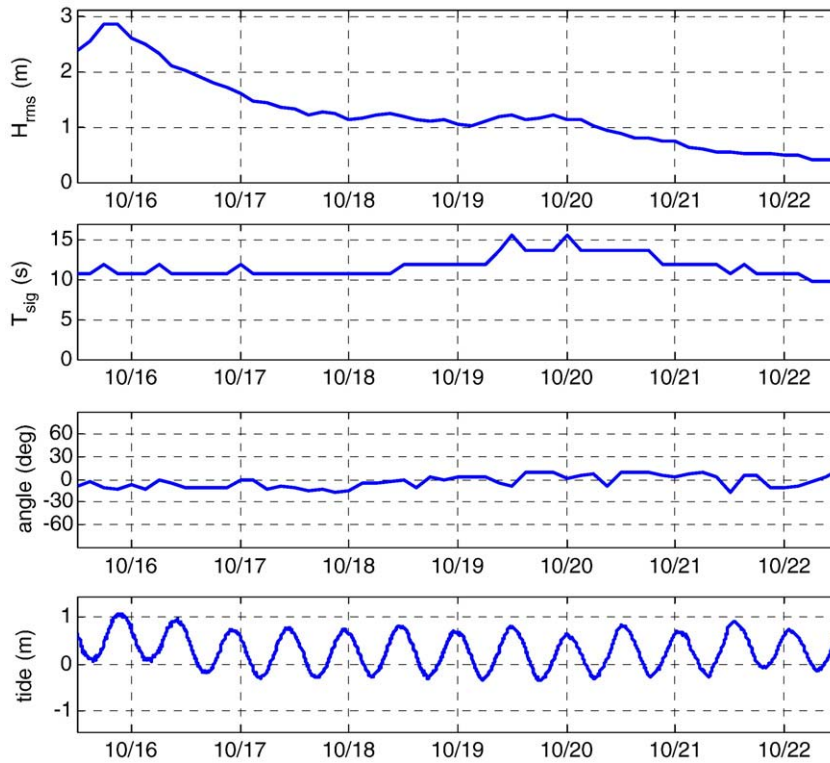
Fig. 4. Observed offshore hydrodynamic conditions for one week during the Duck94 experiment. (H_{rms} is root mean square wave height; T_{sig} is the significant wave period; angle is the peak wave angle of incidence; and tide is the 6-minute average water level.)

and L_y = 20, 40, 80, 160, 320, 640, 1280, 2560 m used in all possible combinations.

2.2. Hydrodynamic observations

The wave and current field was measured at a number of locations in the study area (Fig. 2). Offshore, in 8 m depth (and about 900 m from the shoreline), an alongshore array of pressure sensors

recorded coherent time series used to estimate the frequency-directional spectrum of the wave energy (Pawka, 1983). These data were used to initialize the wave model and derive the summary statistics shown in Fig. 4. At the numerous other locations, there were sensors that measure the pressure field and current velocity (cross-shore and alongshore components) (Elgar et al., 1997; Gallagher et al., 1998). These additional sensors were deployed in a cross-shore array (Fig. 2) and the data are used here to evaluate model prediction errors.

2.3. Nearshore process model

The hydrodynamic conditions were modeled using the integrated Delft3D system (Lesser et al., 2004), that, for the purposes of this study, included wave, water level, and flow simulations. Delft3D uses SWAN (Simulating WAves Nearshore, Booij et al., 1999; Ris et al., 1999), a phase-averaged wave model, to force a flow model that solves the unsteady, shallow-water equations. For a full description of the model, please refer to Chapter 9 of the Delft3D-FLOW users' manual (Stelling and van Kester, 1996) and Lesser et al. (2004). For our analysis, the wave and flow modules were coupled so that results include wave-induced currents, changes in water levels, and wave-current interaction.

The model domain setup utilized three spatial grids: one outer, low resolution domain for the wave model in order to place the unobserved, error-prone lateral boundary conditions far from the study area, a nested high resolution wave domain and a separate high
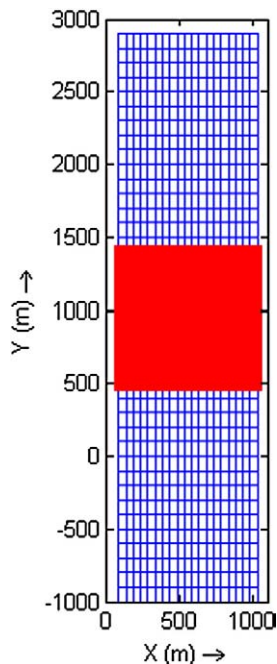

Fig. 5. Coordinate system and grid mesh. The outer wave domain is shown with the coarse mesh and the high resolution wave and flow domains occupy the filled box.

Table 1
Simulation conditions for Duck94 on 19 October 1994

	H_{rms} (m)	T_{sig} (s)	Angle (deg)	Tide (m)
1300 h	1.63	13	10	-0.36
1600 h	1.72	13	10	0.06
1900 h	1.58	15	2	0.63

resolution flow domain. The outer wave grid resolution was 50 m in the cross-shore direction and 100 m in the alongshore direction, and the nested wave and flow grids were 5 m and 20 m in the cross-shore and alongshore directions, respectively (Fig. 5).

Offshore boundary conditions for the wave calculation were provided by directional wave spectra obtained at the 8 m array.

These data were applied uniformly to the offshore and both alongshore boundaries. Applying spatially uniform wave conditions on the alongshore boundaries (where waves should shoal and break as they propagate to the shoreline) is not realistic and introduces model errors. However, these errors do not extend to the inner, nested domains because (1) the alongshore boundaries were
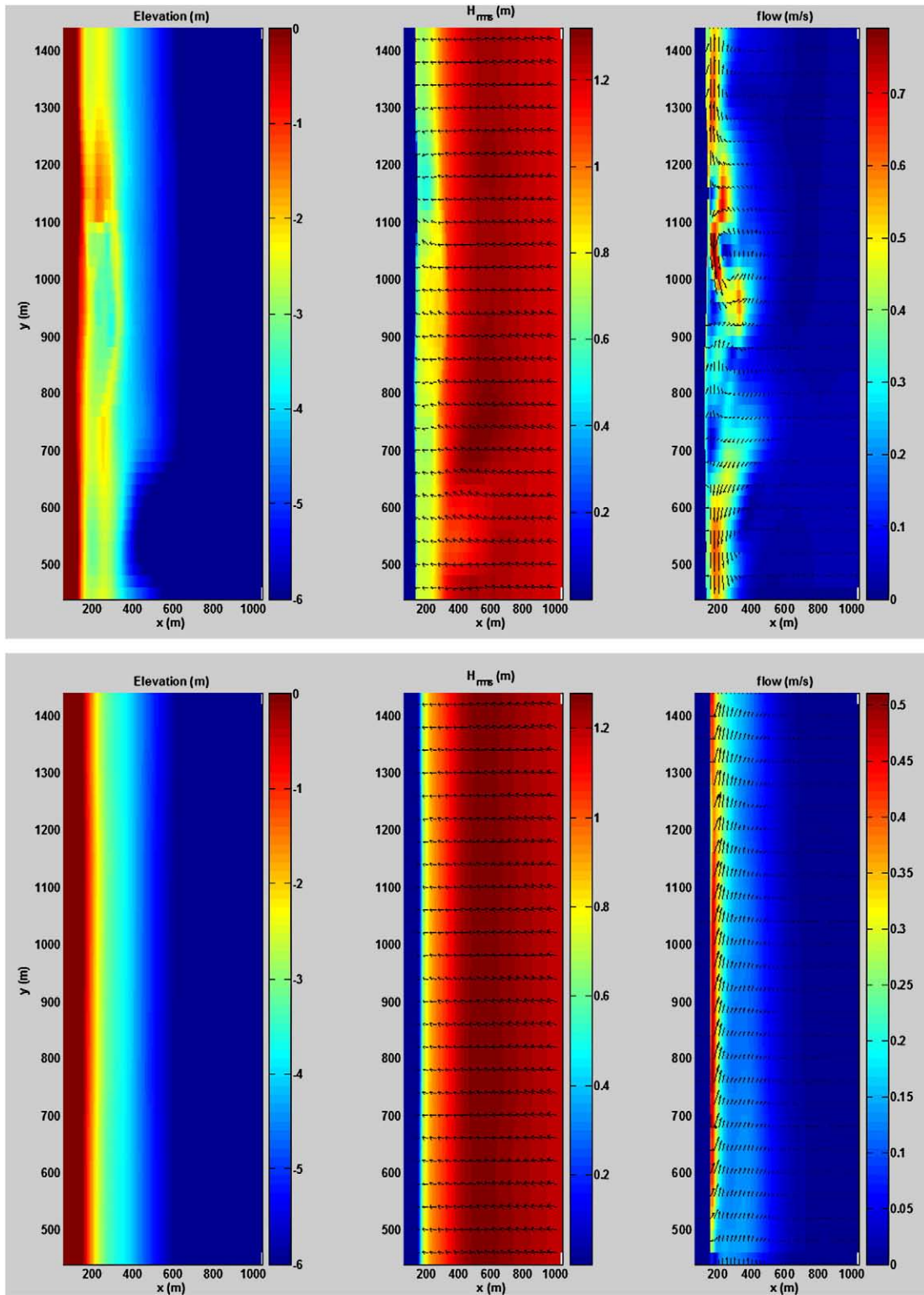

Fig. 6. Input water depth, simulated wave height, and simulated flow speeds computed using very little smoothing (Top panel, $L_x = 5$ m, $L_y = 20$ m) and extreme smoothing (Bottom panel, $L_x = 320$ m, $L_y = 2560$ m). For the wave simulation result, the arrows show the wave direction and the color indicates wave height. For the flow simulation result, arrows indicate flow direction and magnitude while the shading indicates just magnitude. (For interpretation of the references to color in this figure legend, the reader is referred to the web version of this article.)

intentionally placed far from the nested domains and (2) the observed nearly shore-normal wave direction (Table 1) does not allow these boundary errors to propagate toward the central region of the domain. Depth-limited breaking was modeled (Battjes and Janssen, 1978) and required two free parameters (Roelvink, 1993) that control the critical ratio of wave height to water depth ($\gamma = 0.73$) and the intensity of dissipation by a hydraulic jump ($\alpha = 1$). Refraction was modeled, but options to include white capping, wind growth, and quadruplet interactions were not implemented due to the relatively short scale of the overall domain.

Boundary conditions for the flow model were required at the two alongshore boundaries and at the offshore boundary of the flow domain. On the offshore and lateral boundaries, the water level forced to the tide level. Neumann conditions imposed on the lateral boundaries to allow the alongshore components of the flow velocity and water levels to vary consistently with the model physics by constraining only their gradients. No alongshore tidal gradients were imposed, preventing tides from directly driving currents. On the offshore boundary, an absorbing/generating formulation was used (e.g., van Dongeren and Svendsen, 1997) allowing elevation and flow associated with long waves to propagate out of the model domain. Furthermore, model predictions were assumed to represent steady-state conditions. Flow instabilities (Oltman-Shay et al., 1989) were suppressed by using a relatively high bottom friction coefficient (Chezy roughness = 65 which is roughly equivalent to a friction coefficient = 0.0023). Also, long wave motions (Symonds et al., 1982) were not expected because steady wave forcing was used.

The bathymetry was generated as described in Section 2.1, Eq. (4). For each of the filtered bathymetries, Delft3D was executed for a simulation time of 1 h with a time step of 30 s. Collected output was taken from the end of each simulation. Fig. 6 shows model results for two different smoothing scales. Bathymetry that was filtered using the smallest smoothing scales (which did not alter the original high resolution bathymetry) yielded simulations of prominent rip current circulation between $800 < y < 1200$ m and alongshore currents near

lateral boundaries going in opposite directions. In contrast, when using the extremely smoothed bathymetry, alongshore currents increased from south to north (positive y-direction) with minimal changes in cross-shore flow.

3. Results

3.1. Model-data comparison

The model simulations were repeated for 3 different time periods (1300, 1600, and 1900 Hrs EST) on 19 October 1994 during which there was significant modulation in the tide and some modulation of the incident wave conditions (Table 1). These simulations were compared to wave and current observations for the same time periods. Fig. 7 shows the dependence of the root mean square (rms) model-data error on increasing alongshore smoothing scale (while holding the cross-shore smoothing scale at its smallest value). The model-data error was computed by spatially interpolating model results to the observation locations and subtracting this value from the corresponding observed values. These differences were squared and averaged over all observation locations. The rms errors were estimated for wave height (labeled $H_{m,o}$ Error), flow speed (Flow Error) and cross-shore and alongshore components of the flow (U Error and V Error). It is immediately clear that the wave height error behaves differently than the flow error. The wave height error is relatively insensitive to increases in alongshore smoothing scale. The wave height predictions improve (error decreases) when the alongshore smoothing scale increases. These wave height errors appear to be consistent with those of type I in our qualitative classification scheme (Fig. 1), suggesting that alongshore variability at even the largest scales that are resolved by the data are not well resolved by the model. The implication is that the wave model is more skillful when it is provided alongshore uniform bathymetry compared to alongshore variable bathymetry.

The flow errors are substantially more sensitive to alongshore smoothing (Fig. 7). Even though the cross-shore flow component's
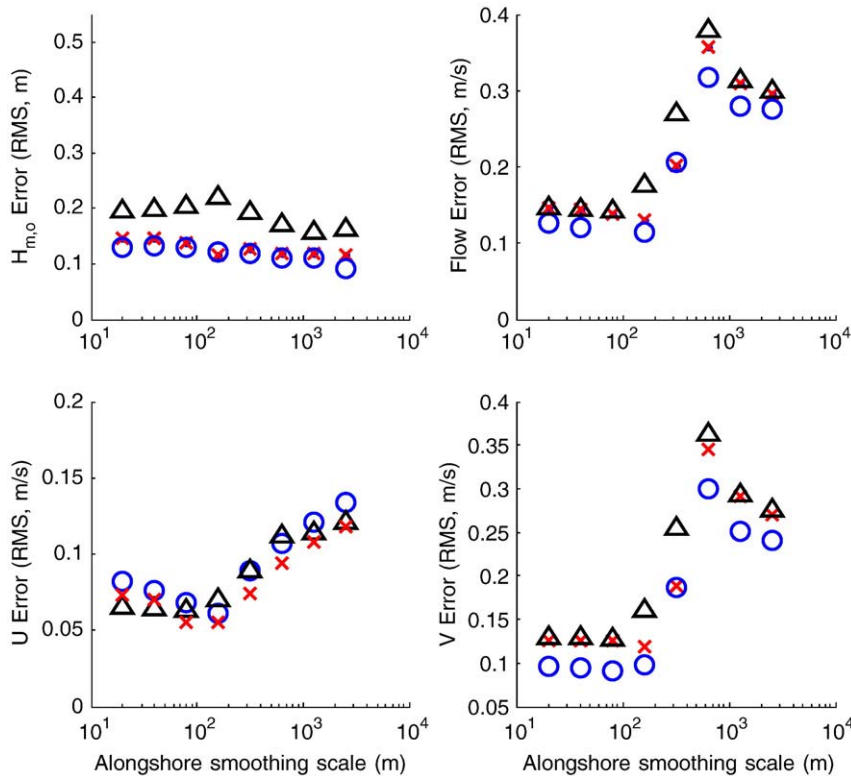

Fig. 7. Model-observation rms errors as a function of alongshore smoothing scale on 19 October 1994 at 1300 (x), 1600 (○), and 1900 (△) hours.
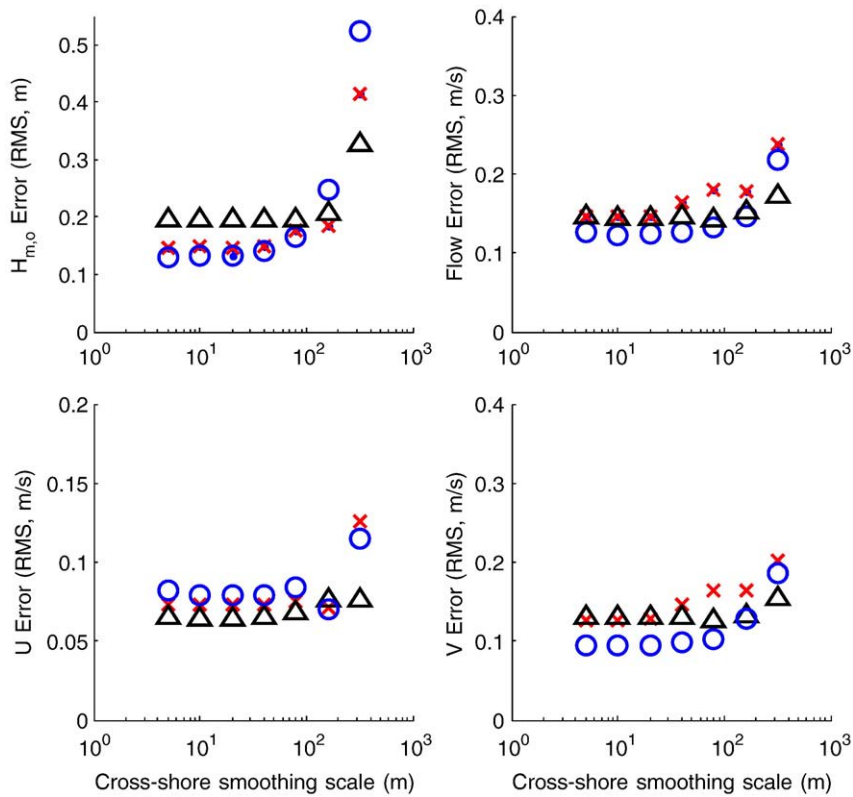
Fig. 8. Model-observation rms errors as a function of cross-shore smoothing. Symbol scheme is same as in Fig. 7.

magnitude is less than that of the alongshore component (note the scale changes in the panels in Fig. 7), the two flow components have similar behavior. The rms error reaches a minimum value with an alongshore smoothing scale of about 100–200 m. This suggests that alongshore features shorter than this are poorly resolved by the bathymetric survey data or are not resolved by the model formulation

(type I errors) and may be removed by filtering the bathymetry in order to achieve a minimum error (type II errors). The flow errors increase rapidly at smoothing scales greater than 200 m, indicating that important features (e.g., crescentic bars associated with rip currents) are removed (type III errors). The error reaches a maximum at a smoothing scale of 640 m and then decreases somewhat before
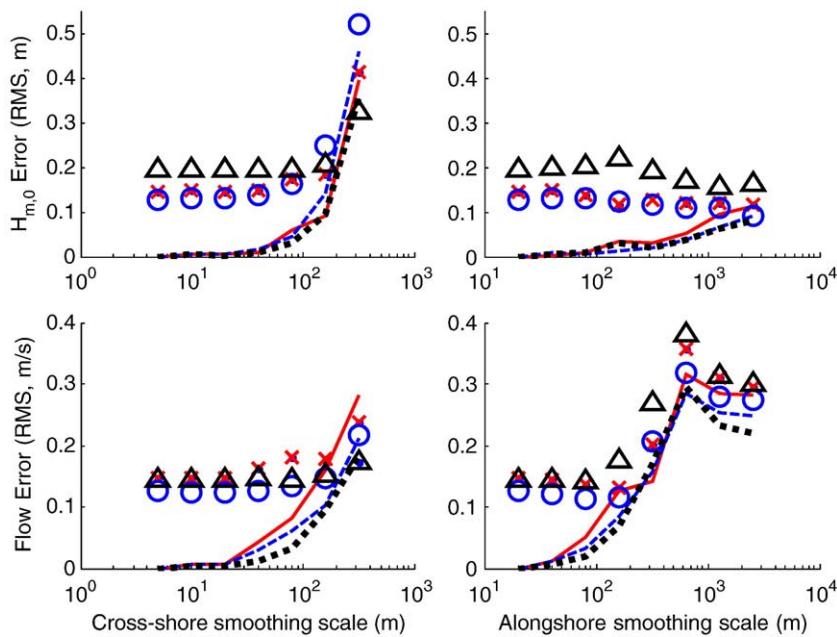

Fig. 9. Comparison of model-model error predictions at 1300 (red solid line), 1600 (blue dashed), and 1900 (black dots) hours to model-data errors (symbols). The left column shows error with respect to cross-shore smoothing, and the right column shows error with respect to alongshore smoothing. The top row shows wave height errors, and the bottom row shows flow errors. Symbol scheme is same as in Fig. 7 for the model-data errors. (For interpretation of the references to color in this figure legend, the reader is referred to the web version of this article.)

leveling off when there are no more interesting features to damage (type IV errors). The local maximum error was not predicted by our qualitative classification scheme (Fig. 1).

For the case of a constant and minimum alongshore smoothing scale (L_y=20 m), we repeated the calculation of wave height and flow errors by varying the cross-shore smoothing scale (Fig. 8). The wave height is insensitive to initial increases in this smoothing scale (which is consistent with type II errors) until L_x>80 m. At this point, the wave height error increases dramatically with increased smoothing as, presumably, the cross-shore bathymetric variations associated with the sandbar are removed (type III errors). The wave height error's response to cross-shore smoothing is shaped similar to the bathymetry error response to smoothing (Fig. 3).

The flow errors are less sensitive to cross-shore smoothing than they are to alongshore smoothing. This suggests that the flow is insensitive to short-scale cross-shore variations in both bathymetry and wave height. It appears that (combining the interpretations of Figs. 7 and 8) accurate flow predictions can be obtained with relatively inaccurate wave height information and even poorly resolved cross-shore bathymetric structure so long as the important alongshore features are well resolved.

3.2. Predicting model errors

As indicated by Eq. (3), optimal use of models and data require that we know the errors of each. One of our objectives is to determine the extent to which we can estimate the damage done by inadequate spatial resolution of bathymetric surveys. To do this, we compared modeled wave height and flow computed with filtered bathymetry to the modeled wave height and flow computed from the highest resolution bathymetry. In this case, we know that model-model errors will be zero at small filter scales, and, assuming the model is somewhat skillful, we expect that model-model errors will increase at the same scales where increases were observed in the model-data comparisons.

Fig. 9 shows the comparison of the high resolution model results to the smoothed model results. The figure also summarizes the cross-shore and alongshore smoothing results from Figs. 7 and 8. At small smoothing scales, the model-model error underestimates the model-data error as expected (Fig. 1). This is due to intrinsic model errors (or observation errors) that cannot be identified from comparing a model to itself. Additionally, there are errors due to unresolved bathymetric features (either larger scale or shorter scale than those resolved by the survey). However, as the smoothing scales increase, the model-model

errors are insensitive in the same range of bathymetric smoothing that the model-data errors were insensitive. The sensitivity to smoothing predicted from the model-model comparison increased at the same filtering scales as was observed in the model-data analysis. Additionally, the strange maximum error observed for the flow at an alongshore smoothing of 640 m is reproduced in the model-model analysis. Thus, the magnitude of the smoothing-induced errors is well predicted in the regions where there is strongest sensitivity (type III errors) and where the largest smoothing scales are applied (type IV errors).

4. Discussion and conclusions

An analysis of nearshore wave and flow model simulations and comparison to observations indicates strong sensitivity to the resolution of input bathymetry. We demonstrated that the sensitivity of wave height and flow models had different characteristics. Wave height predictions were most sensitive to the resolution of cross-shore variability. The sensitivity was, apparently, related to the resolution of sand bars. If the bars were resolved, wave breaking at the bar crests was correctly modeled. Otherwise, filtering of bar-scale bathymetry led to larger errors in the spatial distribution of wave breaking. This led to large errors in wave height predictions. The relative insensitivity of the wave height errors to alongshore smoothing is, perhaps, surprising. This implies that the waves "see" an alongshore-filtered version of the actual bathymetry. In fact, comparing the upper and lower panels of Fig. 6 shows that most of the wave height variation is largely alongshore uniform. This result is likely enhanced for waves that approach nearly shore normal (our case) when the effect of alongshore variability in the bathymetry is not propagated in the alongshore direction.

Flow predictions were most sensitive to the resolution of intermediate scale alongshore variability associated with the prominent rhythmic bars present in the test data set having scales of 200–1000 m. The difference in sensitivity of wave height and flow prediction errors to alongshore variability has been demonstrated by Ruessink et al. (2001), who applied a 1-d profile modeling approach that assumed alongshore uniformity. They showed, using the same data set that we have used, that wave height and flow prediction errors were most accurate when the bathymetry was most alongshore uniform and, therefore, consistent with their model assumptions. However, when the bathymetry became alongshore variable, the wave height prediction error increased only slightly, while the flow prediction error increased substantially.
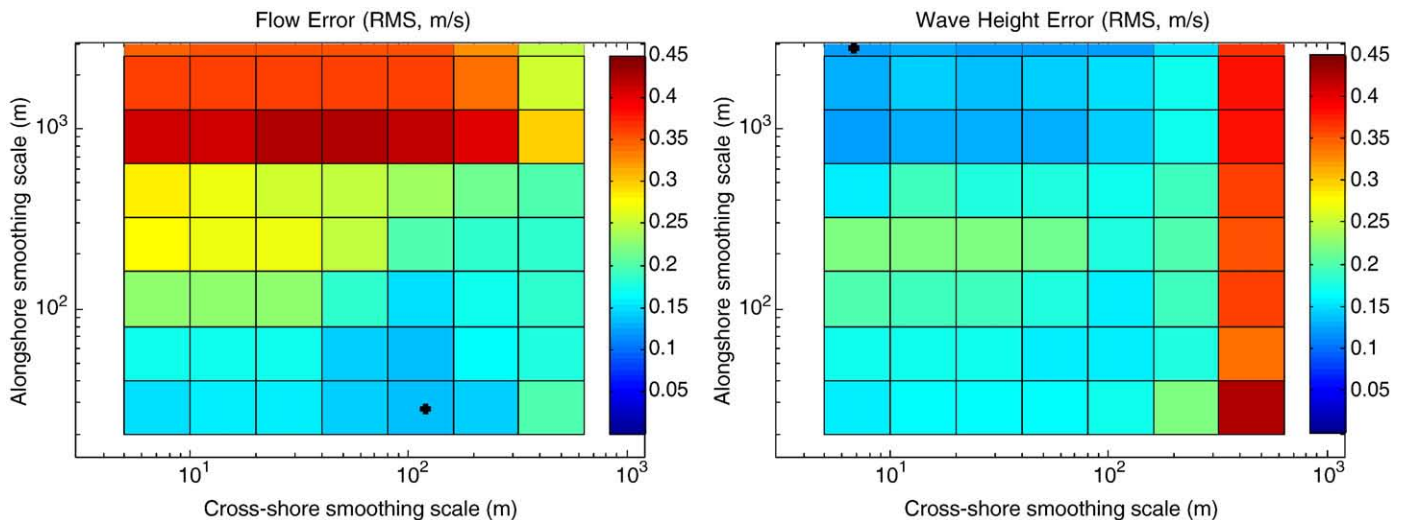

Fig. 10. Difference between modeled and observed flow (left) and wave height (right) as a function of cross-shore and alongshore smoothing scale. The asterisk in each plot marks the smoothing scales of minimum model error for both variables.
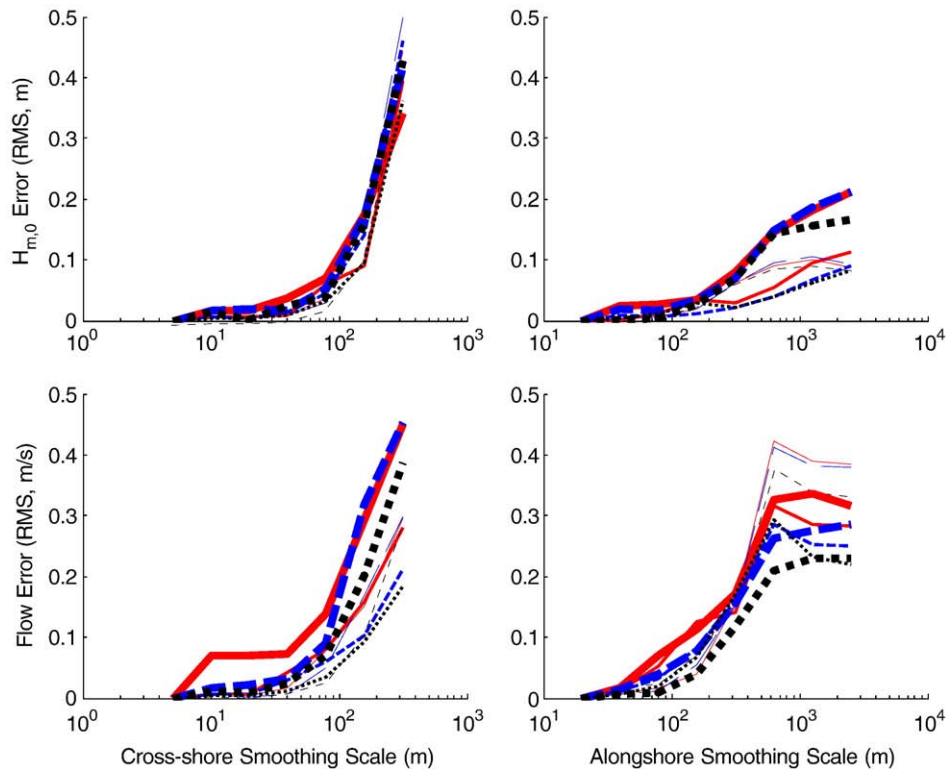
Fig. 11. Comparison of model-model error predictions at 1300 (red solid lines), 1600 (blue dashed), and 1900 (black dots) hours at different alongshore locations (thin: $y=700$ m, medium: $y=930$ m, thick: $y=1200$ m). The left column shows error with respect to cross-shore smoothing, and the right column shows error with respect to alongshore smoothing. The top row shows wave height errors, and the bottom row shows flow errors. (For interpretation of the references to color in this figure legend, the reader is referred to the web version of this article.)

Perhaps the most surprising implication of these results is that the interpolation and smoothing of bathymetry data should be optimized differently for the wave and flow models. Bathymetry used in the wave model can, and perhaps should, include more alongshore smoothing and less cross-shore smoothing than that used in the flow model. Since the wave and flow models utilize numerically different domains anyhow this implementation is relatively straightforward. Fig. 10 shows maps of the flow and wave height errors as a function of both cross-shore and alongshore smoothing scale. The location of the lowest error indicates the optimum smoothing. For the flow prediction, the optimum value is $L_x=80$ m and $L_y=20$ m. (The smallest alongshore scale that we used was 20 m.) For the wave height prediction the optimum value is $L_x=5$ m and $L_y=2560$ m. While a complication in processing inputs for nearshore models, differentiating the treatment of the bathymetric data according to model process will increase the utility of existing data and allow more efficient data collection in the future.

Because the flow and wave height observations were obtained along a single cross-shore transect ($y=930$ m) and because we selected observations that were sampled when there was a large amount of alongshore variability (Fig. 2), it is possible that our results would differ if a different spatial location had been sampled and used in this analysis. For instance, the observations came from a location where the sand bar was relatively far from shore. While data from other locations are not available, it is possible to repeat the model-model comparison at different locations. The model-model comparison approach shown in Fig. 9 was repeated along two other transects at $y=700$ m and $y=1200$ m. These locations included good bathymetric survey data, but were located where the sandbar was much closer to shore, compared with the sensor transect located at $y=930$ m. The general pattern of the additional results (Fig. 11) is similar to those shown in Fig. 9. In fact, the sensitivity of wave height errors to cross-shore smoothing is nearly identical at all locations.

The primary differences in flow errors at different alongshore locations were the values of the maximum RMS error at large smoothing. This variability in sensitivity was already apparent in Fig. 8, where variations in the tide level had an impact on the results. However, the inclusion of other alongshore locations in this analysis indicates that the flow was more sensitive to cross-shore smoothing (particularly at $y=1200$ m, thickest lines) than the primary analysis suggested. A sandbar that was closer to shore and also shallower likely heightened the sensitivity of the model results to both cross-shore and alongshore smoothing. The clear message here is that model predictions are sensitive to smoothing errors and that the sensitivity can vary spatially and temporally.

Finally, we showed that the errors between the observed and modeled flow and wave heights were well predicted when large smoothing scales were applied. This statement was not true for the range of smoothing scales for which the model is insensitive (type I and II errors). In these cases, the predicted errors were, as expected, nearly nil, while there were always model-data errors, even at the lowest smoothing scale. However, the largest, most significant errors (from a forecasting point of view) resulted from the relatively large smoothing scales. This indicates that the damage done by smoothing or from inadequate sampling (which requires smoothing to produce suitable bathymetry for these models) can be learned from model simulations. An application might include estimating the errors that would be incurred from using a 1-d profile model (with alongshore uniform bathymetry) rather than a 2-d resolving model. When high quality data are not available, the model skill is still valuable for making estimates of model errors related to poor resolution of 2-d bathymetry. These error estimates can, for instance, be used in data assimilation applications. Of course, we assume that the 2-d models that are the basis for learning model errors have intrinsically useful skill–there are numerous studies that demonstrate this (Booij et al., 1999; Reniers et al., 2007).

Acknowledgements

References

Battjes, J.A., Janssen, J.P.F.M., 1978. Energy loss and set-up due to breaking of random waves. Proceedings of the 16th Conference on Coastal Engineering, pp. 569–587.

Birkemeier, W.A., Mason, C., 1984. The CRAB: a unique nearshore surveying vehicle. Journal of Survey Engineering 110, 1–7.

Birkemeier, W.A., Thornton, E.B., 1994. The DUCK94 nearshore field experiment. In: Arcilla, A.S., Stive, M.J.F., Kraus, N.C. (Eds.), Proc. Coastal Dynamics '94. ASCE, Barcelona, pp. 815–821.

Booij, N., Ris, R.C., Holthuijsen, L.H., 1999. A third generation wave model for coastal region: 1. model description and validation. Journal of Geophysical Research 104 (c4), 7649–7666.

Elgar, S., Guza, R.T., Raubenheimer, B., Herbers, T.H.C., Gallagher, E.L., 1997. Spectral evolution of shoaling and breaking waves on a barred beach. Journal of Geophysical Research 102 (c7), 15797–15805.

Gallagher, E., Guza, R.T., Elgar, S., 1998. Observations of sand bar evolution on a natural beach. Journal of Geophysical Research 103 (C2), 3203–3215.

Kalman, R.E., 1960. A new approach to linear filtering and prediction problems. Transactions of the ASME-Journal of Basic Engineering 82 (Series D), 35–45.

Lesser, G.R., Roelvink, J.A., Kestera, J.A.T.M.v., Stelling, G.S., 2004. Development and validation of a three-dimensional morphological model. Coastal Engineering 51, 883–915.

Oltman-Shay, J., Howd, P.A., Birkemeier, W.A., 1989. Shear instabilities of the mean longshore current, 2. Field data. Journal of Geophysical Research 94 (C12), 18031–18042.

Ooyama, K.V., 1987. Scale-controlled objective analysis. Monthly Weather Review 115, 2479–2506.

Pawka, S., 1983. Island shadows in wave directional spectra. Journal of Geophysical Research 88 (C4), 2579–2591.

Plant, N.G., Holman, R.A., 1997. Intertidal beach profile estimation using video images. Marine Geology 140, 1–24.

Plant, N.G., Holland, K.T., Puleo, J.A., 2002. Analysis of the scale of errors in nearshore bathymetric data. Marine Geology 191, 71–86.

Press, W.H., Teukolsky, S.A., Vetterling, W.T., Flannery, B.P., 1992. Numerical Recipes in C: the art of scientific computing. Cambridge University Press, Cambridge. 994 pp.

Reniers, A.J.H.M., MacMahan, J.H., Thornton, E.B., Stanton, T.P., 2007. Modeling of very low frequency motions during RIPEX. Journal of Geophysical Research 112 (cc07013). doi:10.1029/2005JC003122.

Ris, R.C., Holthuijsen, L.H., Booij, N., 1999. A third generation wave model for coastal regions: 2. verification. Journal of Geophysical Research 104 (c4), 7667–7681.

Roelvink, J.A., 1993. Dissipation in random wave groups incident on a beach. Coastal Engineering 19, 127–150.

Ruessink, B.G., Miles, J.R., Feddersen, F., Guza, R.T., Elgar, S., 2001. Modeling the alongshore current on barred beaches. Journal of Geophysical Research 106 (C10), 22451–22463.

Stelling, G.S., van Kester, J.A.T.M., 1996. A non-hydrostatic flow model in cartesian coordinates, WL|Delft Hydraulics report.

Symonds, G., Huntley, D.A., Bowen, A.J., 1982. Two-dimensional surf beat: Long wave generation by a time-varying breakpoint. Journal of Geophysical Research 87 (C1), 492–498.

van Dongeren, A.R., Svendsen, I.A., 1997. Absorbing-generating boundary condition for shallow water models. Journal of Waterway, Port, Coastal and Ocean Engineering 123 (6), 303–313.